Influence of Magnetoacoustic Oscillations on Electromagnetic Excitation of Shear Acoustic Waves*

M. R. Gaerttner and B. W. Maxfield†
Laboratory of Atomic and Solid State Physics, Cornell University, Ithaca, New York 14850
(Received 12 June 1972)

An oscillatory, nonlocal contribution to the electromagnetic generation of shear acoustic waves in metals has been observed when the magnetic field is perpendicular to the propagation direction. Previous observations of electromagnetic generation of shear acoustic waves have been limited to the field being parallel to the propagation direction. Our observations are explained by considering forces on the lattice that arise from both the directly induced skin-depth electric field and the electric fields due to Gantmakher-splash current sheets.

The electromagnetic excitation of acoustic waves in metals has been observed in the nonlocal limit of electrical conductivity only for shear waves in zero magnetic field or, when a steady field H is present, for shear waves propagating *parallel* to H.[1-4] In this Letter, we report the first observation of electromagnetic excitation of shear waves when the magnetic field is *perpendicular* to the propagation direction. In this geometry, the nonlocal generation efficiency depends upon the conduction-electron dynamics in a very dramatic way; the generation efficiency exhibits an oscillatory magnetic field dependence. This behavior is to be contrasted with the nearly monotonic field dependence that is observed for shear waves propagating parallel to H.

As in the case of conventional magnetoacoustic oscillations in the attenuation, the oscillations in the generation efficiency are also periodic in $1/H$. However, the origin of the generation-efficiency oscillations is not a simple attenuation effect. The following discussion shows that they are due to an interference between a surface shear force and forces arising from current sheets created in the bulk of the conducting specimen at even multiples of the cyclotron radius R_c beneath the surface. These current sheets have precisely the same origin as those giving rise to the field-parallel Gantmakher size effect and are often referred to as Gantmakher splashes.[5]

Depending upon the excitation field orientation, the direction and magnitude of the steady magnetic field and the magnitude of ql ($q = 2\pi/\lambda$ is the acoustic wave vector and l is the carrier mean free path), a variety of acoustic modes may be produced by electromagnetic excitation. In the limit of local conductivity where a magnetic field is necessary, the polarization excited is parallel to the Lorentz force acting upon the induced (eddy) currents, and the acoustic wave amplitude is proportional to the Lorentz force. In the nonlocal limit, transverse acoustic waves having a polarization direction parallel to the induced electric field can be excited in the absence of a steady magnetic field. When a magnetic field is applied and nonlocal conductivity conditions prevail, the situation is much more complex. If H is parallel to the surface as shown in Fig. 1(b), it is ob-

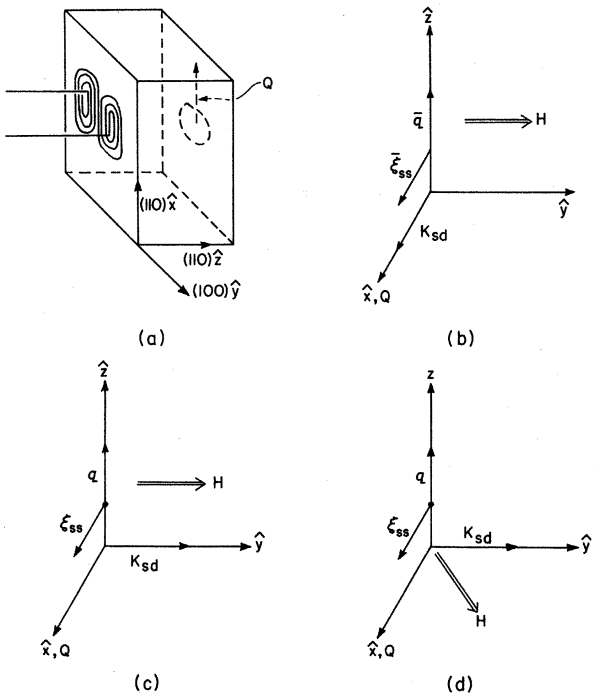

FIG. 1. (a) Relative orientation of rotatable coil, quartz transducer, and specimen crystal axes for (b). The coil used in our measurements had nine straight parallel wires in the central region which was the only area that excited acoustic waves that were detectable by the quartz transducer. K_{sd} is parallel to the central windings. (b)–(d) Three field orientations which result in dramatically different magnetic field dependences for electromagnetic generation.

served that the amplitude of the resulting transverse acoustic wave oscillates periodically in $1/H$.

Measurements were performed on a high-purity single crystal of silver having a residual resistance ratio of 1400; it was oriented so that the normal to the two large faces was within 1° of a ⟨110⟩ direction. One flat face was chemically polished to eliminate the small amount of surface damage that results from the hand lapping which is necessary for achieving adequate surface parallelism and flatness. The other face was left in the as-lapped condition to facilitate bonding a 10-MHz AC-cut quartz transducer.

An efficient double spiral coil shown in Fig. 1(a) was used for electromagnetic excitation of the acoustic waves. This type of coil generates a linearly polarized acoustic wave having a uniform acoustic intensity over the central region to which the quartz transducer is sensitive. From other experiments, it has been observed that signals exhibit the expected exponential decay regardless of whether the coil or quartz transducer is used to excite the acoustic waves.

The quartz transducer was bonded to the sample so that it was sensitive only to the slow shear wave. An electromagnet-Dewar system was used for these measurements; the magnetic field direction could be rotated in a manner such that it was always perpendicular to $\vec{q}$. Figure 1 shows the various orientations of the coil (which could be rotated in the Dewar), sample, and magnetic field that were involved. Pulse-echo techniques involving typical pulse widths of 2 μsec were used for these measurements. All quantitative data were taken at 4.2°K, although qualitative results were obtained as the sample slowly warmed.

For simplicity in the discussion that follows, a number of vectors are defined in Fig. 1. $\vec{K}_{sd}$ is the skin-depth current density and is parallel to the wires of the coil. ξ_{ss} is the amplitude and polarization of the slow shear wave and is always parallel to $\vec{Q}$, the polarization direction of the quartz transducer.

With $H \perp \xi_{ss}$ [Fig. 1(b)], about ten magnetoacoustic oscillations in the attenuation (therefore $ql \simeq 30$) were observed at 48 MHz when transmitting and receiving with the quartz transducer. The upper dashed curve in Fig. 2 shows the measured attenuation of the slow shear wave as a function of $1/\lambda H$ at 48 MHz. As expected, the attenuation is periodic in $1/\lambda H$. The measured period is related to the Fermi momentum p_F. We find $p_F = 1.2\times10^{-19}$ g cm/sec, a number that corresponds roughly to the minimum dimension of the belly orbit and is in excellent agreement with previous, more accurate magnetoacoustic attenuation measurements.[6]

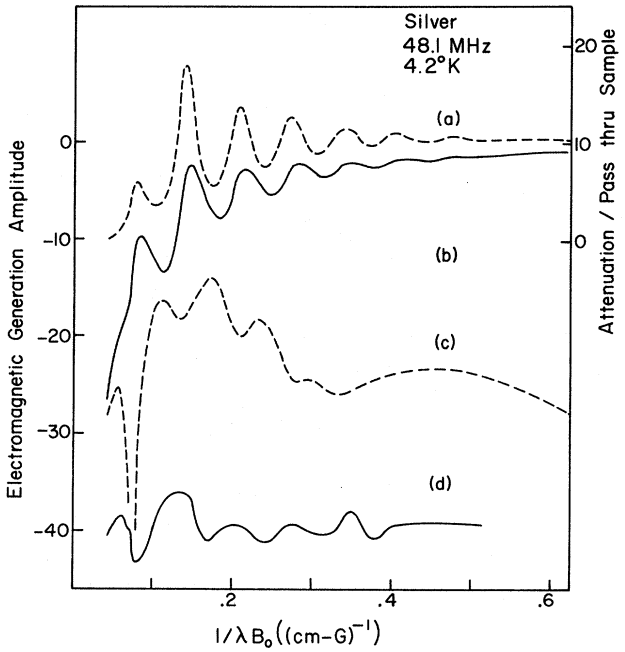

FIG. 2. Curve a, magnetic field (B_0) dependence of the slow shear-wave attenuation (right-hand scale) with $H \perp \xi_{ss}$; curve b, electromagnetic generation (EG) with $H \perp q$, as shown in Fig. 1(b), *after* attenuation of the acoustic wave though the specimen has been taken into account; curve c, EG with H at 45° to ξ_{ss}, as shown in Fig. 1(d); and curve d, EG with $K_{sd} \perp Q$ and H either parallel or perpendicular to K_{sd}, as shown in Fig. 1(c). The signal-to-noise ratio was approximately unity for d. Both scales are in dB; the reference level (0 dB) for the amplitudes is the zero-field value. The sample thickness is 0.43 cm.

With $H = 0$ and using the coil for excitation [$K_{sd} \parallel Q$, as shown in Fig. 1(b)], the expected electromagnetic generation signal was observed using the quartz transducer. With H applied perpendicular to ξ_{ss}, the acoustic signal undergoes oscillations as H is increased. These oscillations cannot be explained completely by the known oscillations in the acoustic attenuation. That is, there is an oscillatory contribution to the process of electromagnetic generation. The upper solid curve in Fig. 2 shows the amplitude of electromagnetic generation as a function of $1/\lambda H$ *after* attenuation changes have been taken into account. Electromagnetic generation has the same period in $1/\lambda H$ as the magnetoacoustic attenuation but the phase is slightly different. Similar attenuation and electromagnetic generation results were

obtained at 10 and 28 MHz.

Measurements involving other relative orientations of the magnetic field and coil (induced current) were also made. With the magnetic field oriented parallel to the polarization of the acoustic wave, that is with $K_{sd} \parallel \xi_{ss} \parallel H \parallel Q$, an expected monotonic decrease of the electromagnetic generation signal with increasing field is observed. In zero field with $K_{sd} \perp Q$, no signal could be detected. In this case, only the fast shear wave, to which the quartz transducer is not sensitive, is generated. With $K_{sd} \perp Q$ and a magnetic field applied either parallel or perpendicular to K_{sd}, the observed signal is reduced by about 40 dB, as shown by the lower solid curve in Fig. 2. However, as shown in the lower dashed curve in Fig. 2, electromagnetic generation is observed in an oblique magnetic field; the oscillations are a mixture of periods resulting from contributions of a number of carrier orbits having different Fermi-surface dimensions.

Qualitatively, when the sample was allowed to warm up, the oscillatory field dependence disappeared quickly, but, as expected, the zero-field electromagnetic generation signal did not decrease as rapidly. Such behavior is expected because the number of magnetoacoustic oscillations increases approximately linearly with l for $ql \gg 1$, while the zero-field electromagnetic generation becomes relatively independent of mean free path once $ql > 1$.

The general theory presented by Quinn[7] perhaps includes the problem studied here although we have carried out no detailed analysis. Even if this analysis were done, it would be limited to a free-electron metal. Below we present a qualitative description of our observations which implicitly takes into account the effects of the shape of the Fermi surface.

The oscillations in electromagnetic generation are believed to result from interference between forces generated within the skin depth and forces generated by Gantmakher splashes[5]; this is illustrated in Fig. 3. Since the magnitude of progressively higher-order splashes decreases rapidly, the significant contribution must come from the first one or two splashes.

In an acoustic medium having a free surface, the amplitude of an acoustic wave generated by a force $F(z)$ is given by

$$\xi(z) = (\rho s \omega)^{-1} e^{iqz} \int_0^\infty F(z_0) \cos q z_0 \, dz_0.$$

Let us consider only one Gantmakher splash and assume that for our purposes the forces can be

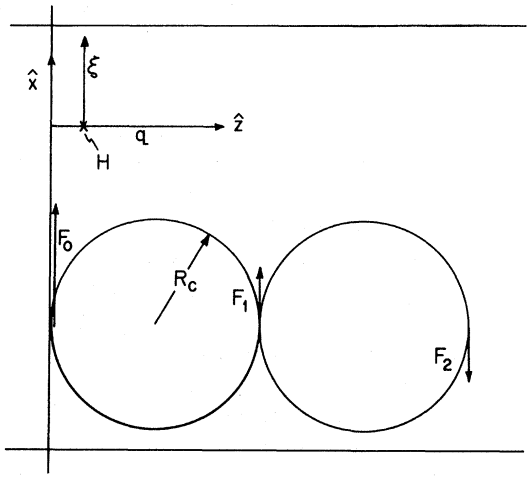

FIG. 3. Model used to explain the oscillatory electromagnetic generation. In a magnetic field, extremal orbit carriers (their trajectories are shown as circles) create Gantmakher-splash current sheets beneath the surface.

approximated by highly localized sources, namely,

$$F(z) = F_0(H)\, \delta(z) + F_1(H)\, \delta(z - 2R_c),$$

where δ is the Dirac δ function and $F_0(H)$ and $F_1(H)$ are functions of the magnetic field. From rf size-effect calculations,[8] it follows that the force due to the first splash is in the same direction as the force in the skin-depth region; hence F_0 and F_1 will be of the same sign with

$$|F_1| < |F_0|.$$

The acoustic amplitude resulting from the above force is then

$$\xi = \xi_0(H) + \xi_1(H) \cos 2qR_c,$$

where ξ_0 and ξ_1 are positive field-dependent constants. Maxima in ξ should occur for $2R_c = N\lambda$, where N is an integer. This is also the rough criterion for maxima in the magnetoacoustic attenuation oscillations.

This model is not exact in that it does not consider the influence of nonextremal orbits, the finite skin depth, and the detailed nature of the surface scattering (specular or diffuse). Nonextremal orbits will cause phase shifts in magnetoacoustic oscillations and undoubtedly also cause phase shifts in the electromagnetic generation process. Both the amplitude and phase of electromagnetic generation would be affected by diffuse surface scattering. Since there is probably considerable diffuse surface scattering, a small phase difference between the type of electromag-

netic generation under consideration and the oscillatory attenuation is to be expected.

*Work supported by the U. S. Atomic Energy Commission under Contract No. AT(11-1)-3150, and by the Advanced Research Projects Agency through the Technical facilities of the Materials Science Center at Cornell University, Contract No. MSC 1801.

†Alfred P. Sloan Research Fellow.

[1]B. Abeles, Phys. Rev. Lett. 19, 1181 (1967).

[2]G. Turner, R. L. Thomas, and D. Hsu, Phys. Rev. B 3, 3097 (1971).

[3]W. D. Wallace, M. R. Gaerttner, and B. W. Maxfield, Phys. Rev. Lett. 27, 995 (1971).

[4]Y. Goldstein and A. Zemel, Phys. Rev. Lett. 28, 147 (1972).

[5]V. F. Gantmakher, Zh. Eksp. Teor. Fiz. 42, 1416 (1962) [Sov. Phys. JETP 15, 982 (1962)].

[6]V. J. Easterling and H. V. Bohm, Phys. Rev. 125, 812 (1962).

[7]J. J. Quinn, Phys. Lett. 25A, 522 (1967).

[8]G. E. Juras, Phys. Rev. 187, 784 (1969).

One-Electron Energy Levels in Fe_3O_4

D. L. Camphausen,* J. M. D. Coey, and B. K. Chakraverty

Groupe de Transitions de Phases, Laboratoire de Magnetisme, Centre National de la Recherche Scientifique, 38 Grenoble-Gare, France

(Received 22 June 1972)

A one-electron energy diagram is suggested for magnetite, which is consistent with recent soft-x-ray emission and absorption spectra, cathodoluminescence, and optical-absorption data.

In the $3d$ transition-metal oxides, normal bands of mainly $2p$ oxygen and $4s$ metal (M) character are separated by an energy gap E_g of about 6 eV. The $3d(M)$ electrons interact strongly with each other and with the surrounding anions, giving rise to a set of localized states or else narrow bands in the $2p(O)$-$4s(M)$ gap, which usually contains the Fermi level.

Optical spectroscopists represent the energy of the highly correlated d-electron manifold by a term which may include electrons in different orbital and spin states. An alternative approach is to ignore completely the collective behavior of the d electrons and construct a one-electron energy diagram, as Balberg and Pankove did for Fe_3O_4.[1] Here we wish to suggest a different one-electron energy scheme which we believe is in better agreement with the experimental data.

Two parameters determine the main features of the one-electron energy diagram. One is Δ_{cf} ($=10Dq$), the crystal-field splitting of the t_2 and e one-electron orbitals due to their covalent mixing and electrostatic interaction with the ligands. The other is Δ_{ex}, the Hund's-rule exchange splitting between spin-up and spin-down orbitals on the same cation. Other intra-atomic electrostatic interactions are ignored. Dq may be deduced directly from the optical spectrum of the ion. Limits may be set of Δ_{ex} for a $3d^n$ ion in an octahedral site for $4 \leq n \leq 7$ from a knowledge of the spin state. Essentially there is a high- or low-spin state, depending on whether Δ_{ex} is greater or less than Δ_{cf}.

According to Balberg and Pankove,[1] all the majority-spin d electrons {five spin-down electrons in the tetrahedral (A) sites and ten spin-up electrons in the octahedral [B] sites in $(Fe^{3+})[Fe^{2+}$-$Fe^{3+}]O_4\}^2$ *lie below the top of the 2p(O) band,* and only the eleventh spin-down d electron on the octahedral sites is in the gap E_g. For this they assumed $\Delta_{ex} \simeq 6$ eV, quoting a theoretical value for MnO. They interpret their cathodoluminescence data as showing that the crystal-field splitting of the $3d(B)$ spin-down orbitals lies between 2.6 and 3.2 eV; the degeneracy of the t_{2g} orbitals is partly removed by a trigonal component of the B-site crystal field, and they split into upper e_ϵ and lower a_1 orbitals.

We criticize this scheme for the following reasons: The values of (a) Δ_{ex} and (b) Δ_{cf} are far too large; and (c) it cannot explain the soft-x-ray results. Instead, we propose the scheme of Fig. 1, where *all the occupied d electron levels lie in the gap.*

(a) Exchange splitting: Calculations of the critical value of Δ_{cf} for a transition from a high- to a low-spin state are available in the literature.[3] The transitions occur when $\Delta_{cf} \simeq \Delta_{ex}$, so the calculated values, 17 600 and 30 000 cm^{-1} (2.2 and 3.7 eV) for Fe^{2+} and Fe^{3+}, respectively, are esti-